Inorg. Chem. **2008**, *47*, 736–741

Study of Negative Thermal Expansion and Shift in Phase Transition Temperature in Ti^{4+}- and Sn^{4+}-Substituted ZrW_2O_8 Materials

Klaartje De Buysser,*,† Isabel Van Driessche,† Bart Vande Putte,‡ Paul Vanhee,‡ Joseph Schaubroeck,‡ and Serge Hoste†

Department of Inorganic and Physical Chemistry, Building S3 Ghent University Krijgslaan 281, 9000 Ghent, Belgium, and Faculty of Applied Engineering Sciences, University College Ghent, Schoonmeersstraat 52, 9000 Ghent, Belgium

Received August 23, 2007

The negative-thermal-expansion material ZrW_2O_8 is known to undergo an order–disorder phase transition which affects its expansion behavior. In this study, Ti^{4+} and Sn^{4+} are examined as possible substituting ions for the Zr^{4+} position in ZrW_2O_8. This substitution leads to a decrease in cell parameters, as the ionic radii of the substituents are smaller than the Zr^{4+} ionic radius. A remarkable decrease in transition temperature is noticed. DSC is used to quantify the enthalpy and entropy changes during the phase transition in order to reveal the mechanisms behind this decrease. It is shown that the strength of the M–O bond plays an important role, as it is a partner in the rigid unit mode motion and the order–disorder transition mechanism.

Introduction

ZrW_2O_8 is known as an isotropic negative-thermal-expansion material in its entire kinetic stability range (−273 to 825 °C).[1] This behavior is in contrast with the asymmetry of the vibrational potential well which leads to positive thermal expansion in most solid materials. Contraction upon heating is not exceptional among solids, as it can be seen for example in tetrahedrally bonded crystals at low temperature and β-quartz at high temperatures.[2,3]

ZrW_2O_8 is formed by corner-linked ZrO_6 and WO_4 polyhedra which are connected by two-fold-coordinated oxygen atoms. In the WO_4 tetrahedra, one oxygen atom remains singly coordinated. The polyhedra are arranged in an open-framework structure. RUMs, or rigid unit modes, can occur within these polyhedra. These are low-energy vibrations of the polyhedra without distortion of the intrahedral bond distances or angles. These RUMs have been associated with a possible mechanism behind the large negative thermal expansion behavior exhibited by the ZrW_2O_8 crystal structure.[4−10]

The isotropy of the thermal expansion is caused by the cubic crystal structure of α-ZrW_2O_8 ($P2_13$) with WO_4 tetrahedra aligned along the [111] axis. ZrW_2O_8 undergoes an order−disorder transition at 150−160 °C from cubic α to cubic β ($Pa\bar{3}$). The direction in which the WO_4 tetrahedra point becomes dynamically disordered in the high-temperature phase. The phase transition also affects the thermal expansion coefficient, but the negative thermal expansion is maintained: α-phase $= -10 \times 10^{-6}$ °C^{-1} and β-phase $= -4 \times 10^{-6}$ °C^{-1}.[11]

The use of ZrW_2O_8 to tailor the thermal expansion of composite materials is described in the literature.[12−22]

* To whom correspondence should be addressed. E-mail: Klaartje.DeBuysser@Ugent.be.
† Ghent University Krijgslaan.
‡ University College Ghent.

(1) Evans, J. S. O.; Mary, T. A.; Vogt, T.; Subramanian, M. A.; Sleight, A. W. *Chem. Mater.* **1996**, *8*, 2809.
(2) Taylor, R. E. In *Data series on material properties*, 1st ed.; Ho, Y., Ed.; ASM International: Materials Park, OH, 1998.
(3) Callister, W. D. *XXXXX*, 5th ed.; Anderson, W., Ed.; Wiley and Sons: Danvers, 2000; p 661.
(4) Barrera, G. D.; Bruno, J. A. O.; Barron, T. H. K.; Allan, N. L. *J. Phys.−Condens. Mat.* **2005**, *17*, R217.
(5) Evans, J. S. O.; David, W. I. F.; Sleight, A. W. *Acta Crystallogr. B* **1999**, *55*, 333.
(6) Gallardo-Amores, J. M.; Amador, U.; Moran, E.; Alario-Franco, M. A. *Int. J. Inorg. Mater.* **2000**, *2*, 123.
(7) Noailles, L. D.; Peng, H. H.; Starkovich, J.; Dunn, B. *Chem. Mater.* **2004**, *16*, 1252.
(8) Sleight, A. W. *Inorg. Chem.* **1998**, *37*, 2854.
(9) Allen, S.; Ward, R. J.; Hampson, M. R.; Gover, R. K. B.; Evans, J. S. O. *Acta Crystallogr. B* **2004**, *60*, 32.
(10) Tao, J. Z.; Sleight, A. W. *J. Solid State Chem.* **2003**, *173*, 442.
(11) Mary, T. A.; Evans, J. S. O.; Vogt, T.; Sleight, A. W. *Science* **1996**, *272*, 90.
(12) Kofteros, M.; Rodriguez, S.; Tandon, V.; Murr, L. E. *Scripta Mater.* **2001**, *45*, 369.
(13) Yilmaz, S.; Dunand, D. C. *Compos. Sci. Technol.* **2004**, *64*, 1895.

10.1021/ic701660w CCC: $40.75
Published on Web 12/21/2007

Although the use of ZrW_2O_8 allows tuning of the thermal expansion of the composite materials, the ever-present phase transition represents a drawback. The phase transition temperature (150−160 °C) separates two domains of slightly different expansion coefficients. A ZrW_2O_8−ZrO_2 composite with zero thermal expansion over a very large temperature range is therefore very difficult to synthesize.[14,20,23] Shifting the phase transition temperature could therefore be of great practical importance because it allows in principle to move the disturbing shift in thermal expansion to outside the range of practical application of the material.

Two different mechanisms are published in order to explain the order−disorder transition. The first mechanism is an S_N2-type reaction in which the W−O_{free} bonds are broken followed by the inversion of WO_4 tetrahedra.[24] ^{17}O NMR studies have revealed another mechanism in which it was confirmed that all oxygen atoms present in the structure undergo an exchange even below the phase transition. When the phase transition temperature is reached, adjacent tetrahedra undergo a "ratchet" motion by which all tetrahedra rotate and a mutual exchange between all oxygen sites occurs. This second mechanism implies breaking of the Zr−O bonds involved in the Zr−O−W linkages;[25] therefore, substitution of the Zr^{4+} ion within the ZrW_2O_8 structure is supposed to strongly affect the phase transition temperature.

According to conventional knowledge, the occurrence of substitutional solid solutions requires that the ions that are replacing each other must be similar in size. Candidate substituent ions also match the preferable the charge of the Zr^{4+} ion.[26] $Zr_{1-x}M_xW_2O_8$ solid solutions were obtained by substituting Zr^{4+} ions (86 pm)[27] with other 4+ valency ions such as Sn^{4+}(83 pm)[28] and Hf^{4+} (85 pm). Hafnium tungstate exhibits identical negative thermal expansion properties as ZrW_2O_8, but the phase transition temperature shifts to higher values.[1,25,29,30] In contrast, substitution by Sn^{4+} ions induces a decrease in phase transition temperature.[28] Some trivalent ions such as Y^{3+}, Lu^{3+}, Sc^{3+}, In^{3+}, etc. were also used in substituted $Zr_{1-x}M_xW_2O_{8-\delta}$ materials, yielding a noticeable decrease in phase transition temperature.[31−35]

In this article, we attempt to modulate the phase transition temperature by substituting the Zr^{4+} site in the octahedra with Ti^{4+}. Sn^{4+}-substituted materials were also synthesized to compare our results. Extensive analysis of the substituted materials by X-ray analysis, thermomechanical analysis, and differential scanning calorimetry was used to understand the mechanisms of the phase transition and the parameters which can influence the phase transition temperature.

Experimental Section

$Zr_{1-x}Ti_xW_2O_8$ ($x = 0-0.05$) and $Zr_{1-x}Sn_xW_2O_8$ ($x = 0-0.05$) solid solutions were prepared by a solid-state reaction using commercially available oxides ZrO_2 (>99%) TiO_2 (>99%), SnO_2 (>99.9%) (Aldrich), and WO_3 (>99%) (Acros). These oxide mixtures were pressed at 750 MPa into small bars of 0.3 g (2 mm × 2 mm × 13 mm) after 24 h of tumble-milling in the presence of zirconia pearls. The bars were reaction-sintered for 15 h in a preheated furnace at 1180 °C, followed by quenching in liquid nitrogen to avoid decomposition into the metal oxide precursors.

The thermal expansion properties (α and phase transition temperature) of the ceramic bars were measured with a vertical push rod thermomechanical analyzer (TA Instruments 2940) using a heating rate of 5 °C/min from room temperature to 300 °C under a constant force of 0.5 N. Identification of the different phases present in the powder samples were performed on a X-ray diffractometer D5000 using Cu Kα radiation (Siemens). The XRD powder diffraction data were collected by a step scanning method (2θ range from 10° to 80°). The lattice cell parameters were calculated between 30° and 80° 2θ by a least-square fit after correcting 2θ with Nelson−Riley's method.[36] The IR spectra were collected using a FT-IR spectrometer (Mattson Research Series). TGA analysis is performed using a heating rate of 10 °C/min under dynamic air flow (TA Instruments SDT 2690). DSC measurements were performed on powder samples using a DSC 2910 (TA Instruments) to determine the phase transition enthalpy, phase transition entropy, and phase transition temperature. The measurements were performed under N_2(g) atmosphere (50 mL/min) to improve the heat diffusion in the DSC furnace. The system was allowed to equilibrate at −40 °C for 3 min, followed by heating to 200 °C at 20 °C/min. The standard aluminum pans were nonhermetically closed.

DSC measurements were performed because they render quantitative information concerning the reaction or transition enthalpy and entropy. This can be obtained using three different DSC measurements, as can be seen in Figure 1: (a) Measurement of two empty aluminum pans for correction of any asymmetry in the heat flow of the system; (b) measurement of an empty aluminum pan and a reference material (sapphire) for providing a calibration factor that translates the measured heat flow units (mW) into heat capacity units (J/g·°C); and (c) measurement of

(14) De Buysser, K.; Lommens, P.; De Meyer, C.; Bruneel, E.; Hoste, S.; Van Driessche, I. *Ceram.-Silikaty* **2004**, *48*, 139.
(15) Matsumoto, A.; Kobayashi, K.; Nishio, T.; Ozaki, K. *Thermec'2003, Pts 1−5* **2003**, *426−4*, 2279.
(16) Yilmaz, S. *Compos. Sci. Technol.* **2002**, *62*, 1835.
(17) Yilmaz, S. *J. Phys.−Condens. Mat.* **2002**, *14*, 365.
(18) Holzer, H.; Dunand, D. C. *J. Mater. Res.* **1999**, *14*, 780.
(19) Li, X. C.; Prinz, F.; Seim, J. *Smart Mater. Struct.* **2001**, *10*, 575.
(20) Lommens, P.; De Meyer, C.; Bruneel, E.; De Buysser, K.; Van Driessche, I.; Hoste, S. *J. Eur. Ceram. Soc.* **2005**, *25*, 3605.
(21) Verdon, C.; Dunand, D. C. *Scripta Mater.* **1997**, *36*, 1075.
(22) Sakamoto, A. Matano, T.; Takeuchi, H. *IEICE T. Electron.* **2000**, *E83C*, 1441.
(23) Niwa, E.; Wakamiko, S.; Ichikawa, T.; Wang, S. R.; Hashimoto, T.; Takahashi, K.; Morito, Y. *J. Ceram. Soc. Jpn* **2004**, *112*, 271.
(24) Evans, J. S. O. *J. Chem. Soc. Dalton* **1999**, 3317.
(25) Hampson, M. R.; Hodgkinson, P.; Evans, J. S. O.; Harris, R. K.; King, I. J. Allen, S.; Fayon, F. *Chem. Commun.* **2004**, 392.
(26) West, A. R. In *Solid state chemistry and its applications*; Wiley: Chichester, 1987; p 358.
(27) Shannon, R. D. *Acta Crystallogr. A* **1976**, *32*, 751.
(28) De Meyer, C.; Bouree, F.; Evans, J. S. O.; De Buysser, K.; Bruneel, E.; Van Driessche, I.; Hoste, S. *J. Mater. Chem* **2004**, *14*, 2988.
(29) Nakajima, N.; Yamamura, Y.; Tsuji, T. *J. Therm. Anal. Calorim.* **2002**, *70*, 337.
(30) Yamamura, Y.; Nakajima, N.; Tsuji, T. *Phys. Rev. B* **2001**, art. no. 6418.
(31) Tsuji, T. Yamamura, Y.; Nakajima, N. *Thermochim. Acta* **2004**, *93*, 416.
(32) Hashimoto, T.; Kuwahara, J.; Yoshida, T.; Nashimoto, M.; Takahashi, Y. Takahashi, K.; Morito, Y. *Solid State Commun.* **2004**, *131*, 217.
(33) Nakajima, N. Yamamura, Y.; Tsuji, T. *Solid State Commun.* **2003**, *128*, 193.
(34) Morito, Y.; Takahashi, K.; Wang, S. R.; Abe, H. Katoh, A.; Hashimoto, T. *J. Ceram. Soc. Jpn* **2002**, *110*, 807.
(35) Yamamura, Y.; Kato, M.; Tsuji, T. *Thermochim. Acta* **2005**, *24*, 431.
(36) Nelson, J. B.; Riley, D. P. *Proc. Phys. Soc.* **1945**, *57*, 160.

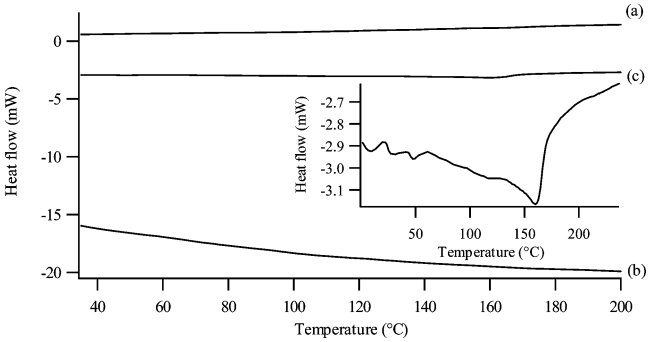

Figure 1. Heat flow measurements of (a) two empty pans, (b) empty pan and reference material (sapphire), and (c) empty pan and sample (pure ZrW_2O_8). The insert gives a detail of the measurement of the sample.

the empty aluminum pan and the sample that results in the heat flow of the sample (mW).

The obtained data files are combined over a temperature range of −40 to 200 °C to calculate the heat capacity of the measured sample using eq 1:

$$C_{p,sample}(T)(J/g\cdot°C) = \frac{C_{p,sapphire}(T)(J/g\cdot°C) \times mass_{sapphire}(mg) \times (q_{sample} - q_0)(mW)}{mass_{sample}(mg) \times (q_{sapphire} - q_0)(mW)} \quad (1)$$

where $C_{p,sample}$ and $C_{p,sapphire}$ are the heat capacities of the sample and reference material, respectively; $mass_{sample}$ and $mass_{sapphire}$ are the weights of the sample and reference material in the aluminum pans, q_0 is the heat flow during the DSC measurement of two empty pans, whereas $q_{reference}$ and q_{sample} are the results of the DSC measurement of an empty pan with an aluminum pan filled with sapphire and the sample, respectively. The heat capacity of sapphire at various temperatures was determined using the following expression (eq 2) calculated by the data published by NIST (SRM 720).[37,38]

$$C_{p,sample}(T)(J/g\cdot°C) = \sum_{n=0}^{n=3} a_n T^n(°C) \quad (2)$$

with $a_0 = 723.16$; $a_1 = 2.31$, $a_2 = -5.10^{-3}$, and $a_3 = 5.10^{-6}$.

The baseline of the heat capacity of the $Zr_{1-x}M_xW_2O_8$ samples was determined by extrapolating the heat capacities in both higher- and lower-temperature ranges excluding the phase transition. The excess heat capacity due to the phase transition was obtained by subtracting the baseline. The transition enthalpies and entropies were defined as the numerical integration of the excess heat capacity according to eqs 3 and 4.

$$\Delta H(J/mol) = \int \Delta C_p \, dT \quad (3)$$

$$\Delta S(J/mol\ K) = \int \frac{\Delta C_p}{T(K)} \, dT \quad (4)$$

Results and Discussion

The successful substitution of Zr^{4+} by Ti^{4+} and Sn^{4+} within the ZrW_2O_8 crystal structure is confirmed by X-ray analysis. Figure 2 shows the reflections of pure ZrW_2O_8, $Zr_{1-x}Ti_xW_2O_8$ (with $x = 0.025$ and 0.05), and $Zr_{1-x}Sn_xW_2O_8$ (with $x = 0.025$ and 0.05). No other reflections beside those belonging

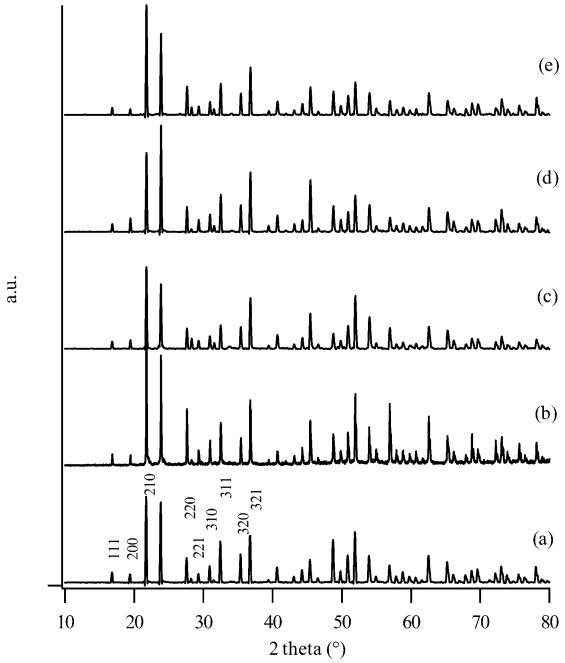

Figure 2. X-ray diffraction patterns of ZrW_2O_8 (a), $Zr_{1-x}Ti_xW_2O_8$ with $x = 0.025$ (b) and 0.05 (c), and $Zr_{1-x}Sn_xW_2O_8$ with $x = 0.025$ (d) and 0.05 (e).

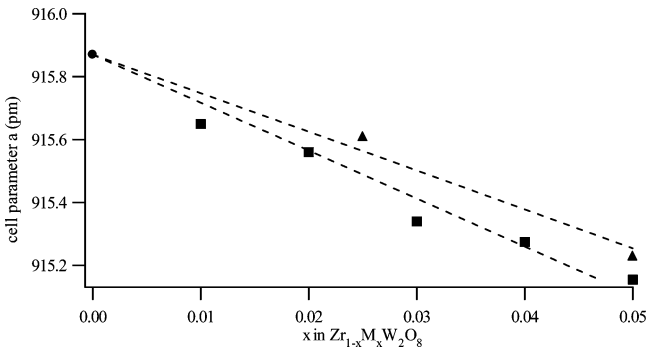

Figure 3. Lattice parameters of ZrW_2O_8 (●), $Zr_{1-x}Ti_xW_2O_8$ ($x = 0.01-0.05$) (■), $Zr_{1-x}Sn_xW_2O_8$ ($x = 0.025-0.05$) (▲).

to pure ZrW_2O_8 are present except for the WO_3 reflections at 28.3° and 31.5° 2θ. The results obtained by X-ray diffraction were used to calculate the cell parameter a of the pure and substituted ZrW_2O_8 materials. The results are shown in Figure 3. A decrease in cell parameter with increasing substitution can be seen in both cases and is attributed to the smaller ionic radii of the substituents in comparison with Zr^{4+}. Ti^{4+} and Sn^{4+} have an ionic radius of 74.5 and 83 pm, respectively, whereas Zr^{4+} has an ionic radius of 86 pm. The decrease in cell parameter is more pronounced in the case of Ti^{4+}-substituted materials, which is nicely linked to the relative sizes. The linear decrease in unit cell parameter with increasing degree of substitution follows Vegard's law strongly, confirming that a solid solution is formed.[26] The solubility limits were reached at $Zr_{0.95}Ti_{0.05}W_2O_8$ and $Zr_{0.8}Sn_{0.2}W_2O_8$.[28,39]

Figure 4 outlines the results for the heat capacity of the ZrW_2O_8 sample measured by DSC analysis. An anomaly in

(37) Archer, D. G. *J. Phys. Chem. Ref. Data* **1993**, *22*, 1441.
(38) Ginnings, D. C.; Furukawa, G. T. *J. Am. Chem. Soc.* **1953**, *75*, 522.
(39) De Buysser, K.; Van Driessche, I.; Vande Putte, B.; Schaubroeck, J.; Hoste, S. *J. Solid State Chem.* **2007**, *180*, 2310.

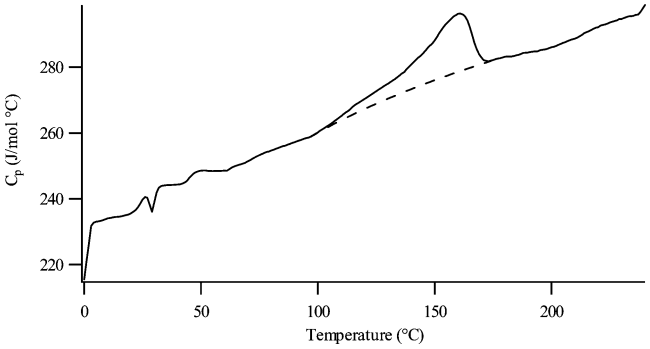

Figure 4. Heat capacity of the ZrW_2O_8 sample.

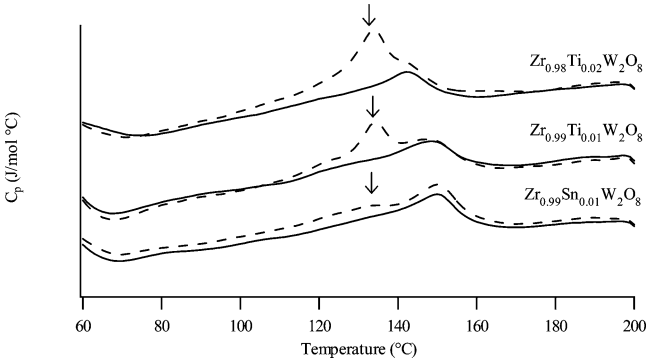

Figure 5. Heat capacity of the substituted materials during first (– – –) and second (—) heat cycle.

the heat capacity (maximum excess: 17.7 J/mol·°C) is seen around 160 °C. This temperature corresponds to the phase transition temperature. The shape of the anomaly in the heat capacity indicates that the α-to-β transition is a λ-type transition typical for a second-order transition.[29−31,40−44] This λ shape indicates that the phase transition starts at temperatures considerably lower than the phase transition temperature. This is in strict correspondence with the variation of the fractional occupancy of the W(1) and W(2) atoms in the two possible tetrahedral orientations along the [1 1 1] diagonal direction as the phase transition is approached. Evans et al. determined this fractional occupancy by Rietveld refinement of neutron powder diffraction data.[5]

DSC measurements were performed for $Zr_{1-x}Ti_xW_2O_8$ ($x = 0.01-0.05$) and $Zr_{1-x}Sn_xW_2O_8$ ($x = 0.025$ and 0.05) and were compared with our results of the pure ZrW_2O_8 sample ($\Delta H = 490.44$ J/mol and $\Delta S = 1.16$ J/mol·K). Some DSC measurements showed two peaks during the first heating cycle. This could be an indication for two transitions. Nevertheless, the peak at 133 °C was no longer detected during a second heating cycle as can be seen in Figure 5. This phenomenon is in the literature attributed to loss of water (confirmed by TGA-MS).[45] TGA on our materials does not indicate loss of water (Figure 6a), nor does IR spectroscopy show the presence of O−H stretching vibrations (Figure 6b). The TGA trace shows a little increase in weight due to buoyancy effects. During the synthesis, the materials are submitted to extreme cooling from 1180 to −200 °C, so it is not unrealistic to think that they show internal stresses which are released at 133 °C during the first heating cycle. Therefore, all samples are annealed at 220 °C before the actual recording of the heat flow data starts.

The phase transition temperature is examined for the substituted materials. A comparison between the data obtained by TMA (minimum in the thermal expansion coefficient) and DSC (maximum in the excess heat capacity diagram) is made in Figure 7. The small differences between the two analysis techniques are due to differences in the samples (powders (DSC) versus bars (TMA)), differences in heat rate (5 °C/min for TMA versus 20 °C/min for DSC), and differences in gas flow (N_2(g) during the DSC experiments versus no gas flow during TMA experiments). The gas influences the thermal equilibration, whereas a higher heating rate will result in an overshoot of the phase transition temperature. Powder measurements exclude the influence of porosity or cracks present in the bars. Notwithstanding these differences, a remarkable correspondence between TMA and DSC data was found. Both techniques reveal a decrease in phase transition temperature with increasing Ti^{4+} and Sn^{4+} substitution. As illustrated by Figure 5 for the second heat cycle, the maximum in the heat capacity plot shifts to lower temperatures due to the substitution by Ti^{4+} and Sn^{4+}. This effect is more strongly present in the case of substitution by Sn^{4+} ions. The thermal expansion properties were also screened with TMA, and the results are given in Figure 8. The thermal expansion coefficients are measured in a fixed temperature range: for the α-phase [25−100 °C] and β-phase [200−300 °C]. No significant differences can be seen after substitution.

The evolution of the phase transition enthalpy with degree of substitution is given in Figure 9. A decrease in phase transition enthalpy is noticed as the degree of substitution increases. The decrease is more pronounced for the Sn^{4+}-substituted materials, which can be understood from the lower Sn−O bond strength (531.8 ± 12.6 kJ/mol vs Ti−O, 672.4 ± 9.2 kJ/mol), which facilitates the ratchet motion, breaking of the M−O bonds, and lowers the phase transition temperature. The DSC measurements prove that the thermodynamic parameters indeed vary with different degrees of substitution. It is clear that our findings support a transition mechanism in which a ratchet motion of tetrahedra is involved. Indeed, the alternatively proposed mechanism only involves breaking of the W−O bond and its thermodynamics would not be affected by substitution at the Zr^{4+} position.

This realization led us to investigate other substituted ZrW_2O_8 materials published in the literature. An increase in phase transition temperature (Hf^{4+} substitution) is indeed linked with a larger Hf−O bond dissociation energy in comparison with Zr−O. The higher phase transition temperature is stated by Nakajima[29] to be linked to a smaller

(40) Yamamura, Y.; Nakajima, N.; Tsuji, T. *Solid State Commun.* **2000**, *114*, 453.
(41) Stevens, R.; Linford, J.; Woodfield, B. F.; Boerio-Goates, J.; Lind, C.; Wilkinson, A. P.; Kowach, G. *J. Chem. Thermodyn.* **2003**, *35*, 919.
(42) Hushur, A.; Shabbir, G. Ko, J. H.; Kojima, S. *J. Phys. D−Appl. Phys.* **2004**, *37*, 1127.
(43) Hashimoto, T.; Katsube, T.; Morito, Y. *Solid State Commun.* **2000**, *116*, 129.
(44) Yamamura, Y.; Tsuji, T. Saito, K.; Sorai, M. *J. Chem. Thermodynam.* **2004**, *36*, 525.
(45) Hashimoto, T.; Morito, Y. *J. Ceram. Soc. Jpn.* **2002**, *110*, 823.

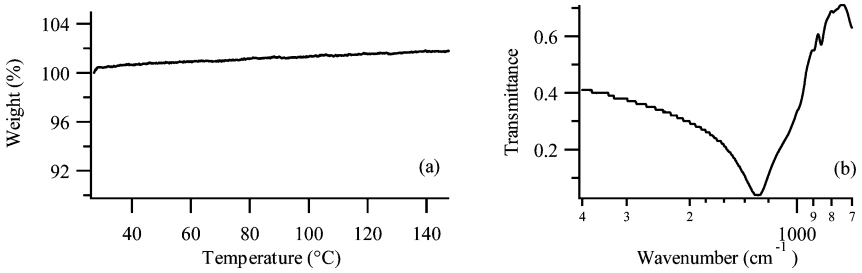

Figure 6. TGA analysis of ZrW_2O_8 (a). IR spectroscopy of $Zr_{0.97}Ti_{0.03}W_2O_8$ (b).

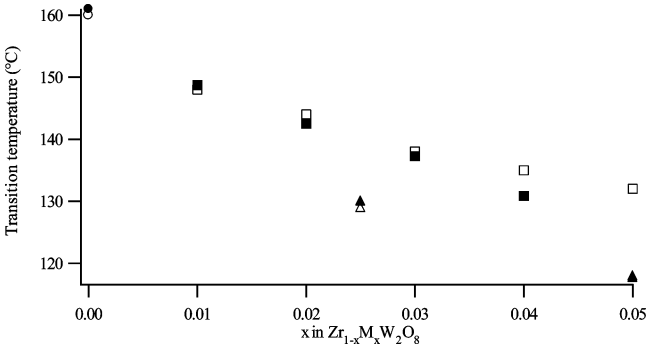

Figure 7. Comparison between T_{tr} obtained by TMA (hollow figures) and T_{tr} obtained by DSC (filled figures). ZrW_2O_8 (●), $Zr_{1-x}Ti_xW_2O_8$ (▲) and $Zr_{1-x}Sn_xW_2O_8$(■).

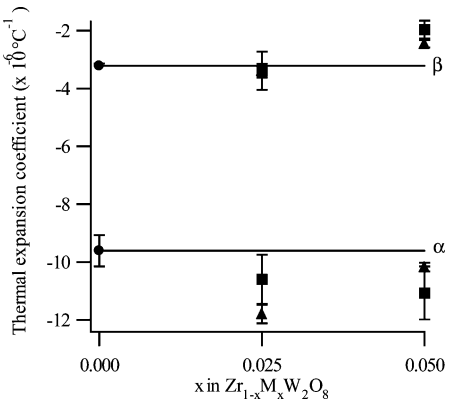

Figure 8. Thermal expansion coefficient of ZrW_2O_8 (●), $Zr_{1-x}Ti_xW_2O_8$ (▲), and $Zr_{1-x}Sn_xW_2O_8$ (■) (α- and β-phase).

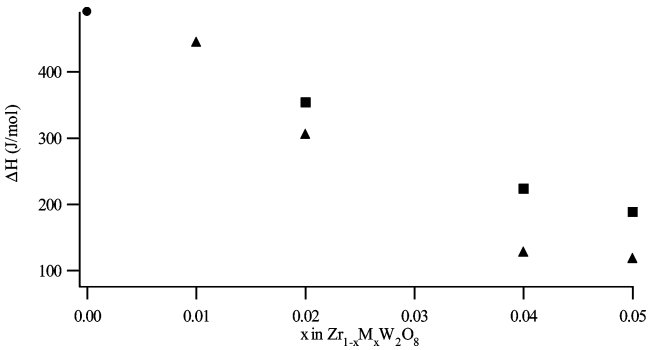

Figure 9. Phase-transition enthalpies of substituted $Zr_{1-x}M_xW_2O_8$ materials: ZrW_2O_8 (●), $Zr_{1-x}Ti_xW_2O_8$ (▲), and $Zr_{1-x}Sn_xW_2O_8$ (■).

free lattice volume. It can be understood that a smaller lattice free volume makes it more difficult for the polyhedra to undergo the ratchet motion and a higher phase transition temperature is necessary. The authors do not take the differences in bond dissociation energy into account. In the

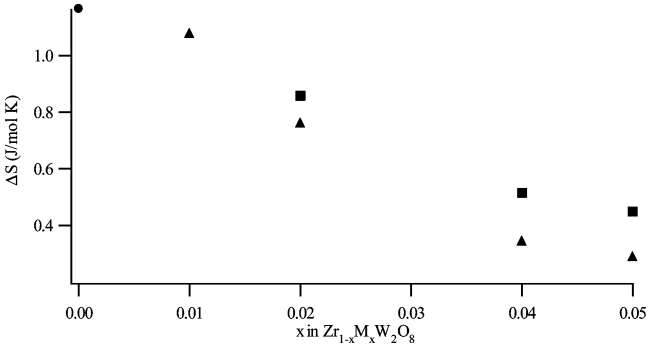

Figure 10. Phase-transition entropies of substituted $Zr_{1-x}M_xW_2O_8$ materials: ZrW_2O_8 (●), $Zr_{1-x}Ti_xW_2O_8$ (▲), and $Zr_{1-x}Sn_xW_2O_8$ (■).

case of Hf, it can be concluded that the increase in phase transition temperature is two-fold: the smaller lattice free volume and the stronger dissociation energy result in an increase of the phase transition enthalpy. For the Ti−O substitution, the lattice free volume was examined and published by us.[39] A decrease in lattice free volume can be seen when the substitution degree is increased, which is similar to the Hf substitution. In both cases, the Zr site is substituted by an ion with a smaller ionic radius. For Ti-substituted solid solution, a decrease in lattice free volume is now accompanied by a decrease in phase transition temperature. The bond dissociation energy of the Ti−O bond is smaller than the Zr−O bond. When taking into account the two factors influencing the phase transition temperature, a decrease is expected due to the differences in bond dissociation energy and an increase due to the smaller lattice free volume. As can be seen from Figure 10, the effect of decreased bond dissociation energy is more pronounced, resulting in an overall decrease of the phase transition temperature in the case of Ti and Sn substitution.

The phase transition entropy changes are mentioned in Figure 10. The positive value for the entropy change results from disordering of the orientation of the two WO_4 tetrahedrons lying along the [1 1 1] direction, as mentioned above in Figure 6. It is stated by Pryde[46] that the available space for the two WO_4 tetrahedrons in the β phase suggest that only two orientations can be taken into consideration. This would mean that the entropy for the phase transition is expected to be R ln 2 (5.8 J/mol·K). If the two tetrahedrons could independently take the two possible orientations, the entropy change would shift to R ln 4 (11.5 J/mol·K). However, the value measured by this DSC experiment

(46) Pryde, A. K. A.; Hammonds, K. D.; Dove, M. T.; Heine, V. J. Gale, D.; Warren, M. C. *J. Phys.−Condens. Mat.* **1996**, *8*, 10973.

reveals a lower value for ΔS_{tr} (20% of R ln 2). Other studies by adiabatic scanning calorimetry[40] have also indicated a discrepancy from the theoretical value due to the difficulty in preparing a complete ordered sample without the presence of a distorted phase before the phase transition. As the magnitude of the experimental value lies closer to R ln 2 than to R ln 4, the order−disorder transition is supposed to be the result of the two WO_4 tetrahedrons along the [1 1 1] with only two conformations in a concerted manner.

A decrease can be seen as the degree of substitution increases. The effect of substitution by Sn^{4+} ions is again more marked than that of Ti^{4+} ions. Nakajima[29] stated that the entropy value is not affected by Hf^{4+} substitution. On the other hand, Yamamura[35] stressed the presence of locally disordered regions within the ordered α domain. This should result in a smaller entropy increase during the phase transition in comparison with pure ZrW_2O_8. As the degree of substitution increases, the local disorder in the crystal structure increases, and hereby, the entropy change during transition should decrease, as proven experimentally in Figure 10.

Conclusion

Substitution of Zr^{4+} ions by Ti^{4+} and Sn^{4+} was successful and resulted in the synthesis of $Zr_{1-x}Ti_xW_2O_8$ and $Zr_{1-x}Sn_xW_2O_8$ solid solutions with $x = 0.00-0.05$. A steady decrease in lattice parameters could be identified with increasing degree of substitution and was attributed to a smaller ionic radius (74.5 and 83 pm) of the substituting metal. The decrease in phase transition temperature noticed in these solid solutions is thought to result from a lower bond dissociation energy of the Ti−O and Sn−O bond in comparison with the Zr−O bond which compensates for the decrease in free lattice volume.

Calorimetric analysis of the Ti^{4+}- and Sn^{4+}-substituted materials revealed a decrease in transition enthalpy and a decrease of the excess of the heat capacity which leads to a decrease in phase transition temperature. The difference in bond strength between Ti−O and Sn−O is translated in smaller decrease of the reaction enthalpy in the case of Ti^{4+}-substituted materials. A small decrease in transition entropy is also detected in this case. Substitution can distort the crystal structure of the materials locally. As the phase transition is an order−disorder transition, small distortion of the material before the phase transition will lower the transition entropy during transition.

IC701660W